Earthline Journal of Chemical Sciences
E-ISSN: 2581-9003; CODEN: EJCSB4
Volume 13, Number 1, February 2026, Pages 87-98
https://doi.org/10.34198/ejcs.13126.07.087098

A heterofullerene cap having trivalent boron – A DFT treatment

Lemi Türker

Department of Chemistry, Middle East Technical University, Üniversiteler, Eskişehir Yolu No: 1, 06800 Çankaya/Ankara, Turkey
e-mail: lturker@gmail.com; lturker@metu.edu.tr

Abstract

Presently, a potential cap for fullerenes has been designed which possesses trivalent boron at the apex that it has been linked to nitrogens of pyrrole type rings. The structure has been investigated thoroughly within the constraints of density functional theory at the level of B3LYP/6-311++G(d,p). The collected data have revealed that the optimized structure has exothermic heat of formation and favorable Gibbs free energy of formation values. It is thermally favored and electronically stable at the standard states. Various structural and quantum chemical data have been collected and discussed, including IR and UV-VIS spectra. Also "nucleus-independent chemical shift" (NICS) data have been presented for typical rings. The collected data indicate that the peripheral ring is an annulene whereas the other rings are either non-aromatic or antiaromatic.

1. Introduction

Annulenes are monocyclic hydrocarbons that contain the maximum number of non-cumulated or conjugated double bonds, and their derivatives. The conjugated system arises from the alternating pattern of single and double bonds, leading to the delocalization of pi electrons throughout the molecule. Some of the annulenes are aromatic while some antiaromatic or non-aromatic [1-5].

[12]-annulene is planar. The three hydrogens in-between the rings are far enough and do not create any strain for the planar arrangement. For [12]-annulene, the dianion is aromatic and stable at 30°C, while the monoanion is an antiaromatic system and unstable at -50°C [6]. Through many centric and inter/intra molecular perturbations, [12]-annulene can be converted to perturbed form [7,8] which has 12-electron peripheral (heteroannulene) π-system and not a planar structure. It might be embedded into a various classes of compounds such as fullerene or nanotube as a cap. The boron atom acts as a centric atom. A fullerene structure can be constructed in the light of isolated pentagon rule (IPR), etc.

Figure 1 shows [12]-annulene and a perturbed structure from it which possess nitrogen and boron atoms linked to each other.

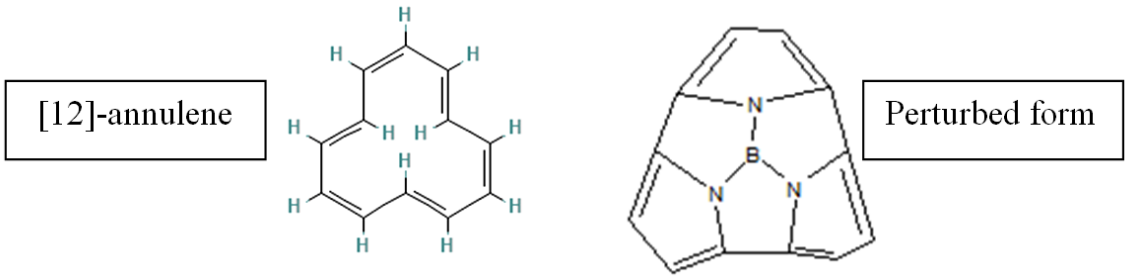

Figure 1. [12]-annulene and a perturbed structure from it.

Received: December 22, 2025; Accepted: January 9, 2026; Published online: January 10, 2026
Keywords and phrases: heterofullerene, boron, annulenes, caps, density functional calculations.

There have many efforts in the use and evaluation of the physical properties of nanomaterials. Fullerenes have attracted keen interest in the past couple of decades [9-11] especially C_{60} and various nanotubes.

According to Euler's theorem these 12 pentagons are required for closure of the carbon network consisting of *n* hexagons and C_{60} is the first stable fullerene because it is the smallest possible to obey this rule. Both C_{60} and its relative C_{70} obey this so-called isolated pentagon rule (IPR). Non-IPR fullerenes have thus far only been isolated as endohedral fullerenes such as $Tb_3N@C_{84}$ with two fused pentagons at the apex of an egg-shaped cage [9] or as fullerenes with exohedral stabilization such as $C_{50}Cl_{10}$ [10] and reportedly $C_{60}H_8$ [11]. Fullerenes with fewer than 60 carbons do not obey isolated pentagon rule (IPR).

In the last couple of decades various structures related to fullerenes, nanotubes etc., have attracted great attention among the scientists especially structural control, and chirality control, remains a significant challenge in the synthesis of single-walled carbon nanotubes (SWNTs) [12]. Also nanotube caps have been studied extensively both theoretically and experimentally [12-17]. Nanotubes have been the focus of interest in many articles published in recent years which concern various aspects of them [18-27].

2. Method of Calculations

In the present study, all the initial optimizations of the structure leading to energy minima have been achieved first by using MM2 method which is then followed by semi empirical PM3 self consistent fields molecular orbital method [28-30]. Afterwards, the structure optimizations have been achieved within the framework of Hartree-Fock and finally by using density functional theory (DFT) at the level of B3LYP/6-311++G(d,p) [31,32]. Note that the exchange term of B3LYP consists of hybrid Hartree-Fock and local spin density (LSD) exchange functions with Becke's gradient correlation to LSD exchange [33]. The correlation term of B3LYP consists of the Vosko, Wilk, Nusair (VWN3) local correlation functional [34] and Lee, Yang, Parr (LYP) correlation correction functional [35]. In the present study, the normal mode analysis for the structure yielded no imaginary frequencies for the $3N–6$ vibrational degrees of freedom, where *N* is the number of atoms in the system. This search has indicated that the molecular structure of considered system corresponds to at least a local minimum on the potential energy surface. Furthermore, all the bond lengths have been thoroughly searched in order to find out whether any bond cleavages occurred or not during the geometry optimization process. All these computations were performed by using SPARTAN 06 program [36]. Whereas the nucleus-independent chemical shift, NICS(0), calculations have been performed by using Gaussian 03 program [37].

3. Results and Discussion

Figure 2 shows the optimized structure of the specie considered. It possesses six 5-membered rings which some of them resemble pyrrole backbone, three of them contain both the nitrogen and boron atoms. The structure could be employed in the construction of certain fullerenes by building hexagonal rings around its periphery within the constraint of IPR rule. In the figure arrow stands for the direction of calculated dipole moment vector. Note that a resultant dipole moment vector is the vectorial sum of the individual bond dipoles, thus location of the heteroatoms greatly affects both the magnitudes and the directions. In the present case, tail of the dipole moment starts from the open-end of the structure and aims at the boron atom.

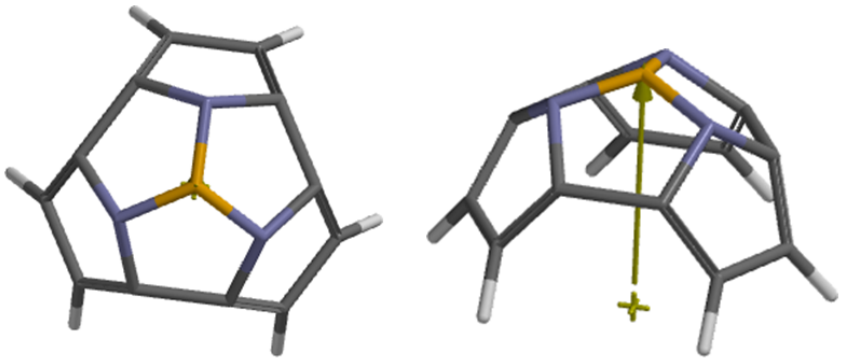

Figure 2. Optimized structure of the specie considered (Two different views).

Figure 3 shows the calculated bond lengths of the structure considered. Note that B-N bonds are about 1.40 Å whereas the bond lengths of the peripheral circuit are alternatingly short and long with respect to each other. Bond lengths of the embedded pyrrole-like rings have sequentially 1.38 Å, 1.45 Å and 1.38 Å in the peripheral ring. The C-N bonds of the pyrrole-like rings are about 1.42 Å. In the light of all these bond length data the peripheral ring appears to be annulene like in character [8].

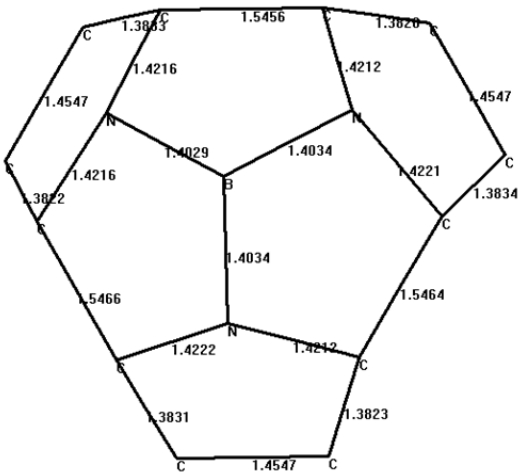

Figure 3. Calculated bond lengths (Å) of the optimized structure considered.

Tables 1 and 2 show, respectively some thermo chemical properties and some energies of the structure presently considered. The data presented in Table 1 reveal that the standard thermo chemical formation data of the specie considered is exothermic (Hº values) and it is favored according to the Gº (Gibbs free energy of formation) value. Some energies of the structure considered are included in Table 2, where E, ZPE and E_C stand for the total electronic energy, zero point vibrational energy and the corrected total electronic energy, respectively. According to the data, the structure is electronically stable. However, note that the structure having twelve peripheral atoms recalls 12-annulene which is an antiaromatic structure.

Table 1. Some thermo chemical properties of the structure considered.

Hº	Sº (J/molº)	Gº
-1706018.744	385.33	-1706133.63

Energies in kJ/mol.

Table 2. Some energies of the structure considered.

E	ZPE	E_C
-1706436.14	407.47	-1706028.67

Energies in kJ/mol.

Figure 4 shows the calculated charges on atoms of the structure considered. It is noteworthy that the ESP charges are obtained by the program based on a numerical method that generates charges that reproduce the electrostatic potential field from the entire wavefunction [36]. Note that the ESP and the natural charges on the boron atom is positive but on the nitrogens are negative but not equal to each other in each case. On the other hand, the total ESP charges of each pyrrole-like ring are -0.539, -0.542 and -0.539 unit of charge which are highly deprived of electron population. As for the natural charges, the respective rings possess charges of -0.826, -0.826 and -0.826.

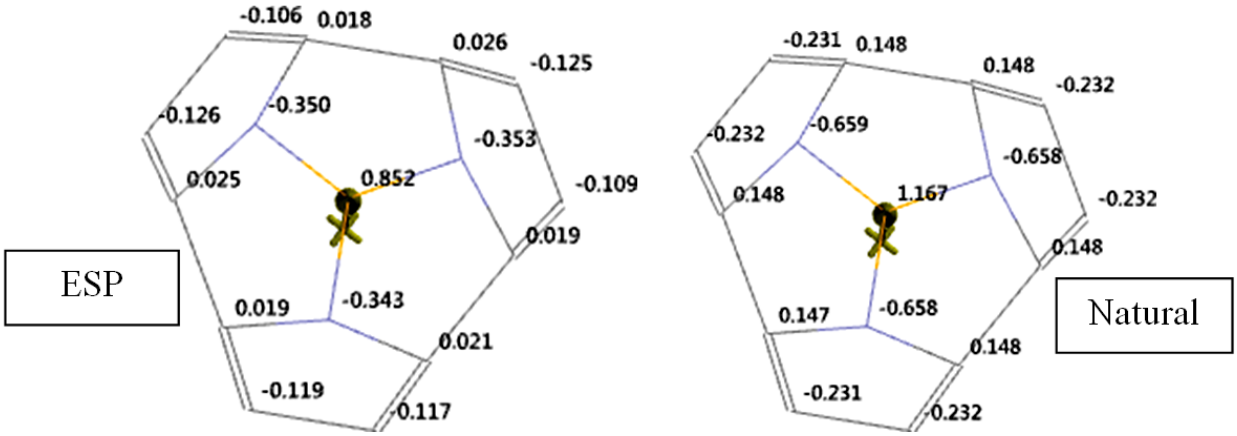

Figure 4. The calculated charges on atoms of the structure considered.

Figure 5 shows the exposed area of the atoms of the structure considered. Note that the exposed surface areas of atoms are highly environment dependent [38]. They differ for the same type of atoms.

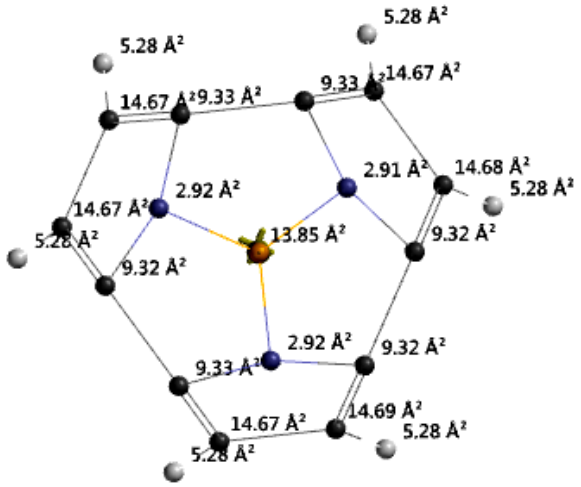

Figure 5. The exposed area of the atoms of the structure considered.

Figure 6 displays the labeling of atoms of the structure of consideration. Table 3 shows some selected Mulliken bond orders and bond lengths for the structure considered.

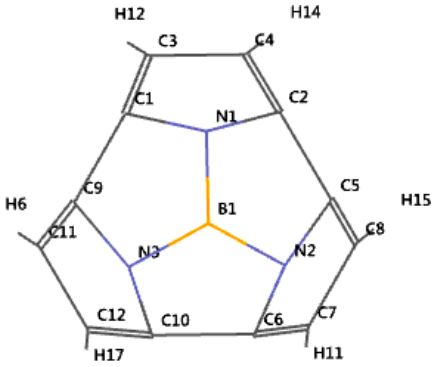

Figure 6. Labeling of atoms of the structure of consideration.

Table 3. Some selected bond orders and bond lengths for the structure considered.

Bond	Mulliken bond order	Bond length and remark
C1C3	1.762	1.3823 [double]
C3C4	1.250	1.4549 [Delco]
C2C4	1.761	1.3824 [double]
C6C7	1.761	1.3824 [double]
C5C8	1.761	1.3828 [double]
C7C8	1.254	1.4549 [deloc]
C2C5	0.735	1.5469 [single]
C6C10	0.737	1.5463 [single]
B1N1	1.042	1.4027 [single]
B1N2	1.040	1.4032 [single]
B1N3	1.041	1.4031 [single]

Figure 7 shows the electrostatic potential map of the structure considered where negative potential regions reside on red/reddish and positive ones on blue/bluish parts of the map. Thus, the peripheral region and the surface region on top of boron atom reside in the positive potential part of the map. However, on the relative bases, the magnitudes on the potential surface are different for those two parts.

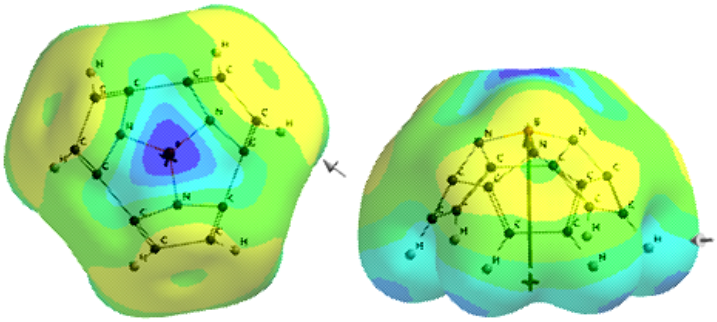

Figure 7. Electrostatic potential map of the structure considered (Two different views).

Figure 8 stands for the local ionization map of the structure considered where conventionally red/reddish regions (if any exists) on the density surface indicate areas from which electron removal is relatively easy, meaning that they are subject to electrophilic attack. Note that the local ionization potential map is a graph of the value of the local ionization potential on an isodensity surface corresponding to a van der Waals surface.

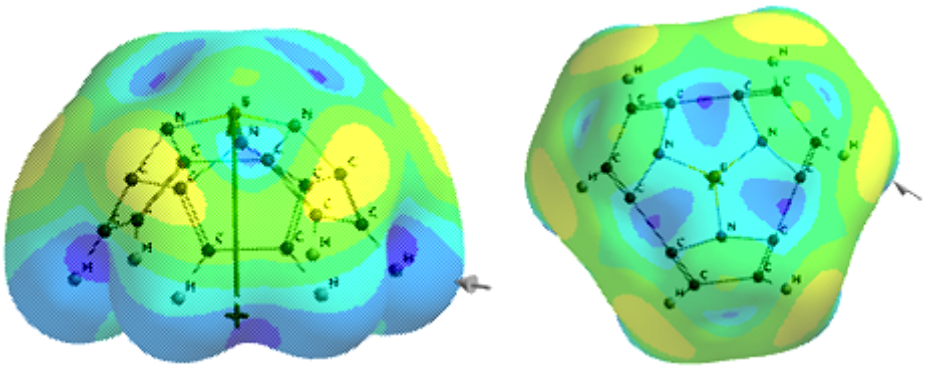

Figure 8. The local ionization map of the structure considered (Two different views).

Figure 9 shows the LUMO map of the structure considered. Note that a LUMO map displays the absolute value of the LUMO on the electron density surface. The blue color (if any exists) stands for the maximum value of the LUMO and the red colored region, associates with the minimum value. It is to be noted that the LUMO and NEXTLUMO (LUMO+1) are the major orbitals directing the molecule towards the attack of nucleophiles [36].

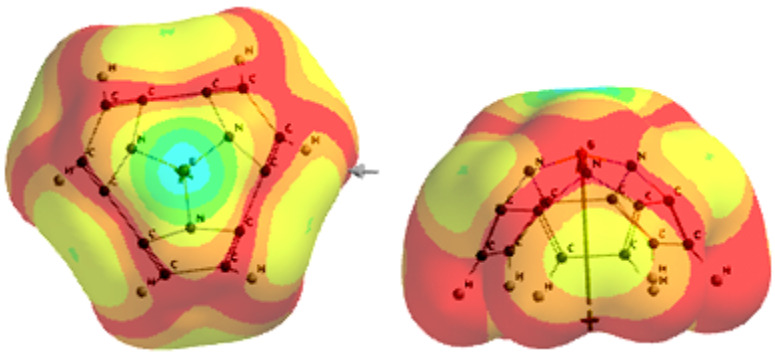

Figure 9. The LUMO map of the structure considered (Two different views).

Figure 10 displays the bond density map of the structure considered. As seen in the figure there exists considerable bond density around the N-B bonds.

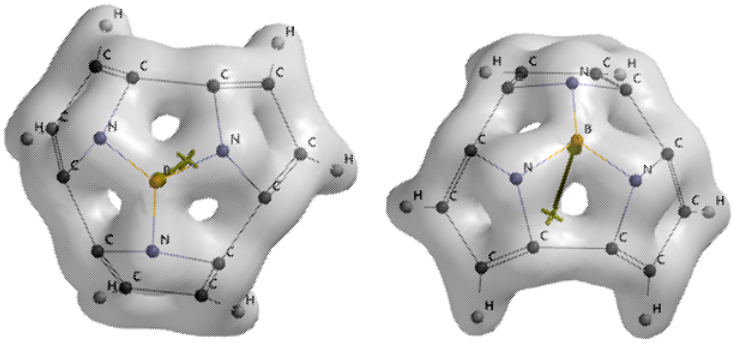

Figure 10. Bond density of the structure considered (Two different views).

Figure 11 shows some of the molecular orbital energy levels of the structure considered. Note that the numbers and energies of the inner lying occupied molecular orbitals are assumed to be responsible for the thermal stability of the compound.

Table 4 lists some properties of the structure of interest. The polarizability is defined according to a multivariable formula which is a function of Van der Waals volume and hardness [36]. The later one is dictated by molecular orbital energies of the highest occupied (HOMO) and the lowest unoccupied (LUMO) molecular orbital energies. It is worth mentioning that the polar surface area (PSA) is defined as the amount of molecular surface area arising from polar atoms (N,O) together with their attached hydrogen atoms.

Table 4. Some properties of the structure of interest.

Dipole	Polarizability	Area (Å²)	Volume (Å³)	PSA (Å²)	Ovality
3.15	57.12	198.28	200.27	8.748	1.20

Dipole moments in debye units . Polarizabilities in 10^{-30} m^3 units.

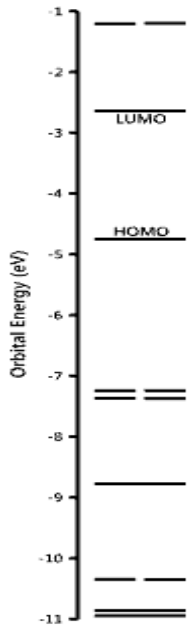

Figure 11. Some of the molecular orbital energy levels of the structure considered.

Table 5 lists some molecular orbital energies of the structure considered. The interfrontier molecular orbital energy gap value, Δε (Δε = ε_{LUMO}-ε_{HOMO}) of the structure is 203.18 kJ/mol.

Table 5. Some molecular orbital energies of the structure considered.

HOMO-1	HOMO	LUMO	LUMO+1
-694.7	-458.23	-255.05	-115.78

Energies in kJ/mol.

Figure 12 displays the HOMO and LUMO (frontier molecular orbitals) patterns of the structure considered. As seen in the figure the HOMO and LUMO orbitals mainly possess π-symmetry. The boron atom does not contribute the HOMO but in great extend to the LUMO.

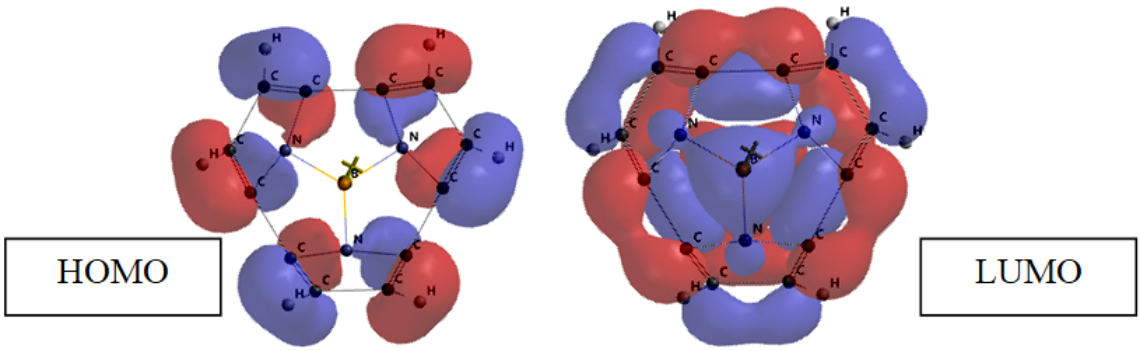

Figure 12. The HOMO and LUMO of the structure considered.

Figure 13 shows the HOMO-1 and LUMO+1 (NEXTHOMO and NEXTLUMO, respectively) of the structure considered. Contribution of the boron atom into the HOMO-1 and LUMO+1 of the structure is nothing.

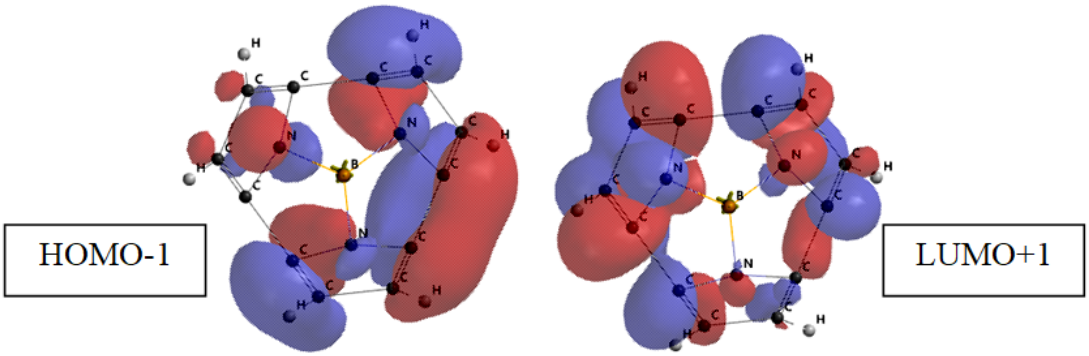

Figure 13. The HOMO-1 and LUMO+1 of the structure considered.

Figure 14 is the calculated IR spectrum of the structure considered. The B-N stretchings occur at 1475 cm^{-1} (assym.) whereas C-H waggings happen at 1529 cm^{-1}. The C=C stretching take place at 1403 cm^{-1}. The symmetric B-N stretchings and ring skeletal breathings overlap at 1259 cm^{-1}.

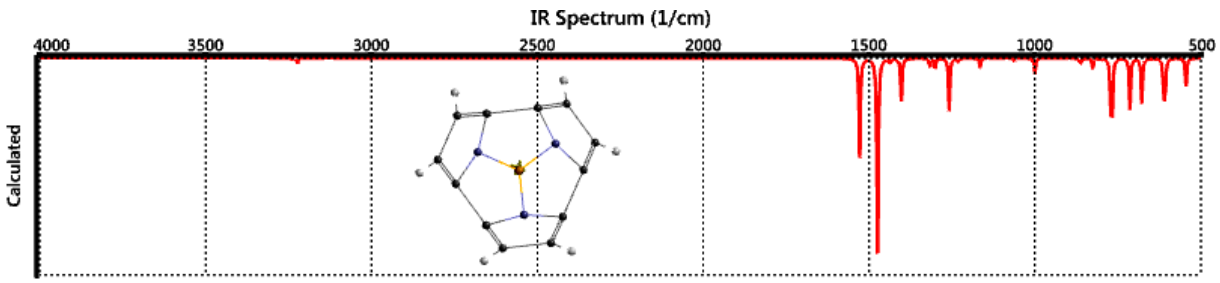

Figure 14. The calculated IR spectrum of the structure considered.

Figure 15 shows the calculated UV-VIS spectrum of the structure considered. The spectrum spreads from the UV region to visible region having λ_{max} values at 348 and 415.71 nm.

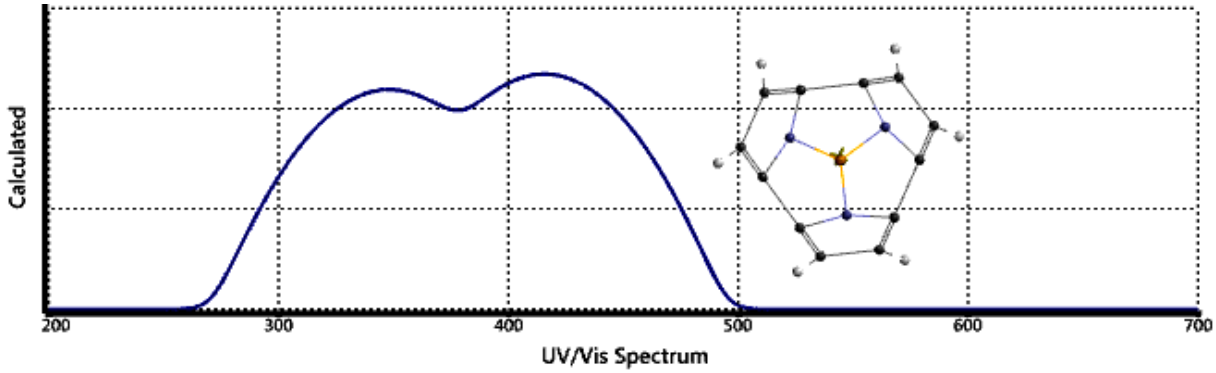

Figure 15. The calculated UV-VIS spectrum of the structure considered.

NICS

NICS is the computed value of the negative magnetic shielding at some selected point in space which is generally, at a ring or cage center [39]. The calculated data piled in the literature through the years indicate that negative NICS values denote aromaticity (-11.5 for benzene, -11.4 for naphthalene) whereas positive NICS values denote antiaromaticity (28.8 for cyclobutadiene) while small NICS values indicate non-aromaticity (-2.1 for cyclohexane, -1.1 for adamantane). NICS may be a useful indicator of aromaticity that usually correlates successfully with the other energetic, structural and magnetic criteria for aromaticity [40-43]. , The NICS has been proved to be an effective probe for local aromaticity of individual rings of polycyclic systems. Several publications exist in the literature that generally aromaticity has been discussed in terms of energetic, structural and magnetic criteria [44-49].

The structure of present consideration consists of six 5-membered rings. However, they fall into two types; having nitrogen atom resembling the pyrrole (type-I) and ones having both the nitrogen and boron atoms (type II). Table 6 has the NICS(0) values of the rings considered.

Table 6. The NICS(0) values of the rings considered.

Type-I	Type-II
4.7802	13.4984

The NICS(0) values of the rings presented in the table reveal that both types of the rings are not aromatic at all (do not conform the Hückel's 4n+2 rule), type -I could be non-aromatic but type-II is definitely antiaromatic. Thus, the presence of boron atom in the structure seems to decrease electron population of pyrrole-like rings as well as the B-N bond having rings.

4. Conclusion

The present computational study has indicated that within the restrictions of DFT treatment at the level of B3LYP/6-311++G(d,p), the designed cap possesses exothermic H^o and favorable G^o values. The structure is electronically stable. The alternating bond length data for the peripheral π-electron circuit is indicative of its annulene like structure. On the other hand, the local aromaticity calculations proves non-aromatic nature of the nitrogen containing 5-membered rings (pyrrole-like rings), whereas the rings having both the nitrogen and boron atoms (B-N bond having rings) are antiaromatic.

References

[1] Carey, F. A., & Sundberg, R. J. (2000). *Advanced organic chemistry* (Vol. 1, pp. 514–524). Kluwer Academic/Plenum Publishers.

[2] Casademont-Reig, I., Ramos-Cordoba, E., Torrent-Sucarrat, M., & Matito, E. (2020). How do the Hückel and Baird rules fade away in annulenes? *Molecules, 25*, 711. https://doi.org/10.3390/molecules25030711

[3] Reginald, H. M., Joseph, S. H. Y., & Thomas, W. D. (1982). Benzannelated annulenes: Toward the understanding of benzannelated annulenes—Synthesis and properties of an [e]-ring monobenzannelated dihydropyrene. *Journal of the American Chemical Society, 104*(9), 2551–2559. https://doi.org/10.1021/ja00373a037

[4] Türker, L. (2003). An ab initio treatment on some isomeric structures of a small pseudocyclacene. Journal of Molecular Structure: *THEOCHEM, 637*(1–3), 109–113. https://doi.org/10.1016/S0166-1280(03)00473-1

[5] Türker, L. (2002). Borazine embedded corannulenes—AM1 treatment. Journal of Molecular Structure: *THEOCHEM, 584*(1–3), 135–141. https://doi.org/10.1016/S0166-1280(02)00012-X

[6] Oth, J. F. M., Rotelle, H., & Schroder, G. (1970). [12]-Annulene. *Tetrahedron Letters, 11*(1), 61–66. https://doi.org/10.1016/S0040-4039(01)87565-1

[7] Dewar, M. J. S. (1969). *The molecular orbital theory of organic chemistry*. McGraw-Hill.

[8] Dewar, M. J. S., & Dougherty, R. C. (1975). *The PMO theory of organic chemistry*. Plenum Press.

[9] Beavers, C. M., Zuo, T., Duchamp, J. C., Harich, K., Dorn, H. C., Olmstead, M. M., & Balch, A. L. (2006). $Tb_3N@C_{84}$: An improbable, egg-shaped endohedral fullerene that violates the isolated pentagon rule. *Journal of the American Chemical Society, 128*(35), 11352–11353. https://doi.org/10.1021/ja063636k

[10] Xie, S. Y., Gao, F., Lu, X., Huang, R. B., Wang, C. R., Zhang, X., Liu, M. L., Deng, S. L., & Zheng, L. S. (2004). Capturing the labile fullerene C_{50} as $C_{50}Cl_{10}$. *Science, 304*(5671), 699. https://doi.org/10.1126/science.1095567

[11] Weng, Q. H., He, Q., Liu, T., Huang, H. Y., Chen, J. H., Gao, Z. Y., Xie, S. Y., Lu, X., Huang, R. B., & Zheng, L. S. (2010). Simple combustion production and characterization of octahydro[60]fullerene with a non-IPR C_{60} cage. *Journal of the American Chemical Society, 132*(43), 15093–15095. https://doi.org/10.1021/ja108316e

[12] Yu, X., Zhang, J., Choi, W., Choi, J.-Y., Kim, J. M., Gan, L., & Liu, Z. (2010). Cap formation engineering: From opened C_{60} to single-walled carbon nanotubes. *Nano Letters, 10*(9), 3343–3349. https://doi.org/10.1021/nl1010178C:\?term=%22Nano+Lett%22[jour]&sort=date&sort_order=desc

[13] Brinkmann, G., Fowler, P. W., Manolopoulos, D. E., & Palser, A. H. R. (1999). A census of nanotube caps. *Chemical Physics Letters, 315*(5–6), 335–347. https://doi.org/10.1016/S0009-2614(99)01111-2

[14] Saito, T., & Saito, H. (2017). Two-way correspondence between carbon nanotubes and caps: Development of a numerical algorithm and a tool for organic cap synthesis. *Carbon, 116*, 678–685. https://doi.org/10.1016/j.carbon.2017.02.038

[15] Ono, S., Takahashi, K., Kubo, R., & Osawa, K. (2016). Relationship between cap structure and energy gap in capped carbon nanotubes. *The Journal of Chemical Physics, 145*(2), 024701. https://doi.org/10.1063/1.4955495

[16] Melle-Franco, M., Brinkmann, G., & Zerbetto, F. (2015). Modeling nanotube caps: The relationship between fullerenes and caps. *The Journal of Physical Chemistry A, 119*(51), 12839–12844. https://doi.org/10.1021/acs.jpca.5b09244

[17] Zhu, Z. P., & Gu, Y. D. (1996). Structure of carbon caps and formation of fullerenes. *Carbon, 34*(2), 173–178. https://doi.org/10.1016/0008-6223(96)00174-1

[18] Sinnott, S. B., & Andrews, R. (2001). Carbon nanotubes: Synthesis, properties, and applications. *Critical Reviews in Solid State and Materials Sciences, 26*(3), 145–249. https://doi.org/10.1080/20014091104189

[19] Harris, P. J. F. (2009). *Carbon nanotube science: Synthesis, properties and applications*. Cambridge University Press. https://doi.org/10.1017/CBO9780511609701

[20] Artyukhov, V., Penev, E., & Yakobson, B. (2014). Why nanotubes grow chiral. *Nature Communications, 5*, 4892. https://doi.org/10.1038/ncomms5892

[21] Pérez-Guardiola, A., Ortiz-Cano, R., Sandoval-Salinas, M. E., Fernández-Rossier, J., Casanova, D., Pérez-Jiménez, A. J., & Sancho-García, J. C. (2019). From cyclic nanorings to single-walled carbon nanotubes: Disclosing the evolution of their electronic structure with the help of theoretical methods. *Physical Chemistry Chemical Physics, 21*(5), 2547–2557. https://doi.org/10.1039/C8CP06615A

[22] Dias, J. R. (2016). Facile calculation of Hückel molecular orbital eigenvalues of short (n,0) nanotubes. *Chemical Physics Letters, 647*, 79–84. https://doi.org/10.1016/j.cplett.2016.01.055

[23] Schwerdtfeger, P., Wirz, L. N., & Avery, J. (2015). The topology of fullerenes. *WIREs Computational Molecular Science, 5*, 96–145. https://doi.org/10.1002/wcms.1207

[24] Gonzalez, S. N. (2008). Boron fullerenes: A first-principles study. *Nanoscale Research Letters, 3*(2), 49–54. https://doi.org/10.1007/s11671-007-9113-1

[25] Dong, H., Lin, B., Gilmore, K., Hou, T., Lee, S.-T., & Li, Y. (2015). B_{40} fullerene: An efficient material for CO_2 capture, storage and separation. *Current Applied Physics, 15*(9), 1084–1089. https://doi.org/10.1016/j.cap.2015.06.008

[26] Türker, L., & Gümüş, S. (2004). An AM1 study on $C_{60}@C_{180}$ system. Journal of Molecular Structure: *THEOCHEM, 674*(1–3), 15–18. https://doi.org/10.1016/j.theochem.2003.12.023

[27] Türker, L. (2003). A theoretical study on the simplest fullerene C_{20}: An AM1 treatment. Journal of Molecular Structure: *THEOCHEM, 625*(1–3), 169–171. https://doi.org/10.1016/S0166-1280(03)00015-0

[28] Stewart, J. J. P. (1989). Optimization of parameters for semi-empirical methods I. *Journal of Computational Chemistry, 10*, 209–220. https://doi.org/10.1002/jcc.540100208

[29] Stewart, J. J. P. (1989). Optimization of parameters for semi-empirical methods II. *Journal of Computational Chemistry, 10*, 221–264. https://doi.org/10.1002/jcc.540100209

[30] Leach, A. R. (1997). *Molecular modeling*. Longman.

[31] Kohn, W., & Sham, L. J. (1965). Self-consistent equations including exchange and correlation effects. *Physical Review, 140*, A1133–A1138. https://doi.org/10.1103/PhysRev.140.A1133

[32] Parr, R. G., & Yang, W. (1989). *Density functional theory of atoms and molecules*. Oxford University Press.

[33] Becke, A. D. (1988). Density-functional exchange-energy approximation with correct asymptotic behavior. *Physical Review A, 38*, 3098–3100. https://doi.org/10.1103/PhysRevA.38.3098

[34] Vosko, S. H., Wilk, L., & Nusair, M. (1980). Accurate spin-dependent electron liquid correlation energies for local spin density calculations: A critical analysis. *Canadian Journal of Physics, 58*, 1200–1211. https://doi.org/10.1139/p80-159

[35] Lee, C., Yang, W., & Parr, R. G. (1988). Development of the Colle–Salvetti correlation energy formula into a functional of the electron density. *Physical Review B, 37*, 785–789. https://doi.org/10.1103/PhysRevB.37.785

[36] Wavefunction, Inc. (2006). SPARTAN 06. Irvine, CA, USA.

[37] Gaussian 03, Frisch, M.J., Trucks, G.W., Schlegel, H.B., Scuseria, G.E., Robb, M.A.,Cheeseman, J.R.,Montgomery, Jr., J.A., Vreven, T., Kudin, K.N., Burant, J.C., Millam, J.M., Iyengar, S.S., Tomasi, J., Barone, V.,Mennucci, B., Cossi, M., Scalmani, G., Rega, N., Petersson, G.A., Nakatsuji, H., Hada, M., Ehara, M., Toyota, K.,Fukuda, R., Hasegawa, J., Ishida, M., Nakajima, T., Honda, Y., Kitao, O., Nakai, H., Klene, M., Li, X.,

Knox,J.E., Hratchian, H.P., Cross, J.B., Bakken, V., Adamo, C., Jaramillo, J., Gomperts, R., Stratmann, R.E., Yazyev, O., Austin, A.J., Cammi, R., Pomelli, C., Ochterski, J.W., Ayala, P.Y., Morokuma, K., Voth, G.A., Salvador, P.,Dannenberg, J.J., Zakrzewski, V.G., Dapprich, S., Daniels, A.D., Strain, M.C., Farkas, O., Malick, D.K., Rabuck, A.D., Raghavachari, K., Foresman, J.B., Ortiz, J.V., Cui, Q., Baboul, A.G., Clifford, S., Cioslowski, J., Stefanov, B.B., Liu, G., Liashenko, A., Piskorz, P., Komaromi, I., Martin, R.L., Fox, D.J., Keith, T., Al-Laham, M.A., Peng, C.Y., Nanayakkara, A., Challacombe, M., Gill, P.M.W., Johnson, B., Chen, W., Wong, M.W., Gonzalez, C., &Pople, J.A., Gaussian, Inc., Wallingford CT, 2004.

[38] Richmond, T. J. (1984). Solvent accessible surface area and excluded volume in proteins: Analytical equations for overlapping spheres and implications for the hydrophobic effect. *Journal of Molecular Biology, 178*(1), 63–89. https://doi.org/10.1016/0022-2836(84)90231-6

[39] Schleyer, P. R., Maerker, C., Dransfeld, A., Jiao, H., & Hommes, N. J. R. E. (1996). Nucleus-independent chemical shifts: A simple and efficient aromaticity probe. *Journal of the American Chemical Society, 118*, 6317–6318. https://doi.org/10.1021/ja960582d

[40] Jiao, H., & Schleyer, P. R. (1998). Aromaticity of pericyclic reaction transition structures: Magnetic evidence. *Journal of Physical Organic Chemistry, 11*, 655–662. https://doi.org/10.1002/(SICI)1099-1395(199808/09)11:8/9<655::AIDPOC66>3.0.CO;2U

[41] Schleyer, P. R., Kiran, B., Simion, D. V., & Sorensen, T. S. (2000). Does $Cr(CO)_3$ complexation reduce the aromaticity of benzene? *Journal of the American Chemical Society, 122*, 510–513. https://doi.org/10.1021/ja9921423

[42] Quinonero, D., Garau, C., Frontera, A., Ballester, P., Costa, A., & Deyà, P. M. (2002). Quantification of aromaticity in oxocarbons: The problem of the fictitious "nonaromatic" reference system. *Chemistry – A European Journal, 8*, 433–438. https://doi.org/10.1002/1521-3765(20020118)8:2<433::AID-CHEM433>3.0.CO;2-T

[43] Patchkovskii, S., & Thiel, W. (2002). Nucleus-independent chemical shifts from semiempirical calculations. *Journal of Molecular Modeling, 6*, 67–75. https://doi.org/10.1007/PL00010736

[44] Minkin, V. I., Glukhovtsev, M. N., & Simkin, B. Y. (1994). *Aromaticity and antiaromaticity: Electronic and structural aspects*. Wiley.

[45] Schleyer, P. R., & Jiao, H. (1996). What is aromaticity? *Pure and Applied Chemistry, 68*, 209–218. https://doi.org/10.1351/pac199668020209

[46] Glukhovtsev, M. N. (1997). Aromaticity today: Energetic and structural criteria. *Journal of Chemical Education, 74*, 132–136. https://doi.org/10.1021/ed074p132

[47] Krygowski, T. M., Cyranski, M. K., Czarnocki, Z., Hafelinger, G., & Katritzky, A. R. (2000). Aromaticity: A theoretical concept of immense practical importance. *Tetrahedron, 56*, 1783–1796. https://doi.org/10.1016/S0040-4020(99)00979-5

[48] Schleyer, P. R. (2001). Introduction: Aromaticity. *Chemical Reviews, 101*, 1115–1118. https://doi.org/10.1021/cr0103221

[49] Cyranski, M. K., Krygowski, T. M., Katritzky, A. R., & Schleyer, P. R. (2002). To what extent can aromaticity be defined uniquely? *Journal of Organic Chemistry, 67*, 1333–1338. https://doi.org/10.1021/jo016255s